Check for updates

Zitierweise: *Angew. Chem. Int. Ed.* **2023**, *62*, e202306511
doi.org/10.1002/anie.202306511

Organic Chemistry

Copper-Phosphido Catalysis: Enantioselective Addition of Phosphines to Cyclopropenes**

Brian S. Daniels[+], Xintong Hou[+], Stephanie A. Corio, Lindsey M. Weissman, Vy M. Dong, Jennifer S. Hirschi,* and Shaozhen Nie**

Abstract: We describe a copper catalyst that promotes the addition of phosphines to cyclopropenes at ambient temperature. A range of cyclopropylphosphines bearing different steric and electronic properties can now be accessed in high yields and enantioselectivities. Enrichment of phosphorus stereocenters is also demonstrated via a Dynamic Kinetic Asymmetric Transformation (DyKAT) process. A combined experimental and theoretical mechanistic study supports an elementary step featuring insertion of a Cu^{I}-phosphido into a carbon-carbon double bond. Density functional theory calculations reveal migratory insertion as the rate- and stereo-determining step, followed by a *syn*-protodemetalation.

Introduction

By inventing strategies to forge C–P bonds, chemists provide entrance to organophosphorus architectures for versatile applications in medicine and catalysis.[1] Among these architectures, the cyclopropyl phosphine motif garners attention because of its distinctive steric and electronic attributes. For example, a cyclic analogue of fosmidomycin shows enhanced antibiotic activity against E. coli, presumably due to restricted rotation.[2] In the realm of catalysis, Takasago's cyclopropyl phosphine ligand, 2,2-diphenylcyclopropylphosphines (cBRIDP) outperforms its 2,2-diphenylvinylphosphines (vBRIDP) in Suzuki–Miyaura cross coupling.[3] Considering ways to construct cyclopropyl phosphines, we focused on hydrophosphination: the direct addition of a P–H bond across a C–C multiple bond.[4] Hydrophosphination represents an attractive and atom-economical platform[5] for controlled synthesis of molecules with stereogenic carbon and/or phosphorous atoms. While progress has been made,[6] stereoselective methods remain rare beyond use of alkynes,[7] oxa-bicycles,[8] and Michael acceptors.[9] Driven by strain release,[10] cyclopropenes show high reactivity,[11,12] and the hydrofunctionalization of cyclopropenes has enabled a direct access to a diverse range of enantiomerically enriched rings.[12] In this report, we disclose enantioselective Cu-catalyzed hydrophosphination to access a range of cyclopropyl-phosphines at ambient temperature. A unique Cu-phosphido mechanism is supported by both experimental and theoretical studies. We provide insights into ligand trends for selectivity using buried volume analysis.

Results and Discussion

Organophosphorous partners bearing P–H bonds with a wide range of acidities (pK_a 9.0 to 22.4)[13] can be activated with transition metal catalysts.[14] For secondary phosphines, coordination followed by deprotonation results in a metal-phosphido complex[9a,c,e–k,15] with high nucleophilicity, and recent studies have revealed impressive versatility of catalytically generated Cu-phosphido complexes.[9e,g–h,15a-e,k-m] Glueck elucidated mechanistic and structural details,[15d,e] while both Glueck and Yin demonstrated catalytic transformations using Cu-phosphidos (Figure 1B).[9g,h] Although Cu- catalyzed hydrophosphination has been studied, both phosphine oxides and phosphites ring-opened to afford allylic phosphine oxides and allylic phosphonates, respectively.[16] At the start of our studies, there was only one transformation, using phosphine oxides and cyclopropenes, that provided the ring-retained cyclopropyl phosphine product, albeit as a racemic mixture.[14l] Coinciding with our efforts, the Wang group was independently pursuing the enantioselective addition of phosphines to cyclopropenes by Pd-catalysis; their asymmetric version occurs by Pd–H insertion into the cyclopropene.[4h] While promising, the scope is limited strictly to ester-bearing cyclopropenes and requires precious metal.[17] While precious metals can be practical on industrial scales,[18] earth abundant metals are more sustainable and economical, while providing an opportunity to uncover novel and complementary reactivity.[19] As an alternative to Pd–H mechanisms, we imagined a strategy involving Cu-phosphido catalysis. In-

[*] B. S. Daniels,[+] X. Hou,[+] Prof. Dr. V. M. Dong
Department of Chemistry, University of California, Irvine
92697 Irvine, CA (USA)
E-mail: dongv@uci.edu
S. A. Corio, L. M. Weissman, Prof. Dr. J. S. Hirschi
Department of Chemistry, Binghamton University
13902 Binghamton, NY (USA)
E-mail: jhirschi@binghamton.edu
Dr. S. Nie
Department of Medicinal Chemistry, GSK
1250 S. Collegeville Rd, 19426 Collegeville, PA (USA)
E-mail: shaozhen.x.nie@gsk.com
[+] These authors contributed equally to this work.

[**] A previous version of this manuscript has been deposited on a preprint server (https://doi.org/10.26434/chemrxiv-2023-3db0j).

© 2023 Wiley-VCH GmbH

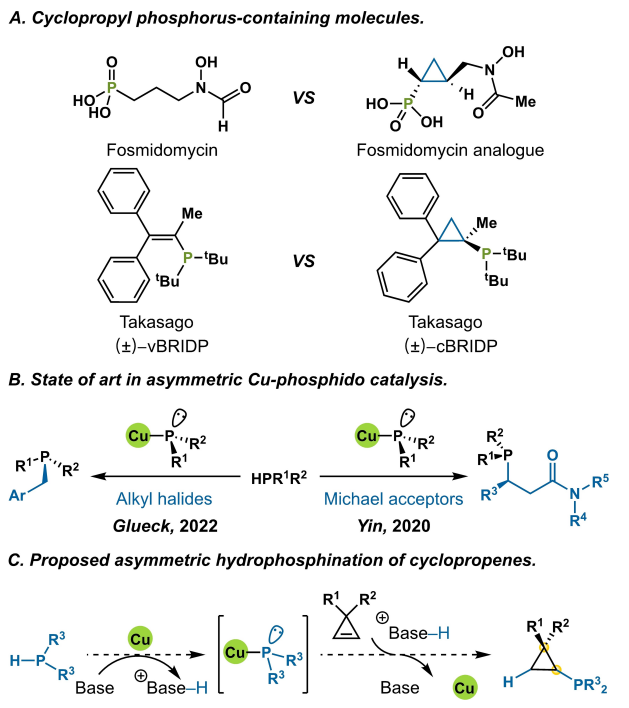

Figure 1. Inspiration of asymmetric hydrophosphination of cyclopropenes: **(A)** Importance of cyclopropyl phosphorus-containing molecules. **(B)** Highlights of previous studies about Cu-phosphido chemistry. **(C)** Our proposed Cu-catalyzed asymmetric hydrophosphination of cyclopropenes.

Table 1: Ligand effects on asymmetric hydrophosphination of **1a**.[a]

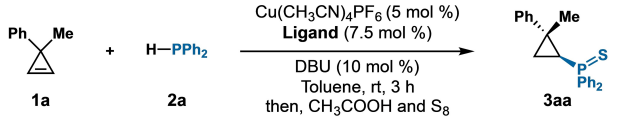

entry	variations	yield (%)	*er*
1	—	92	98:2
2	without $Cu(CH_3CN)PF_6$	—	—
3	without DBU	—	—
4	no (R,R)-^{i}Pr-DuPhos	77	—
5	6 mol% ((R,R)-^{i}Pr-DuPhos	91	79:21
6	**L1** instead of **L5**	90	85:15
7	**L2** instead of **L5**	82	64:36
8	**L3** instead of **L5**	70	90:10
9	**L4** instead of **L5**	73	92:8

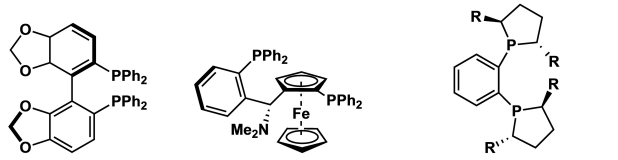

R-SEGPHOS (**L1**) Taniaphos (**L2**) DuPhos R = Me(**L3**), Et(**L4**), ^{i}Pr(**L5**)

[a] Reaction conditions: **1a** (0.12 mmol), **2a** (0.10 mmol), $Cu(CH_3CN)_4PF_6$ (5.0 mol%), ligand (7.5 mol%), DBU (10 mol%), toluene (0.40 mL), 3 h. Yield determined by GC-FID analysis of the reaction mixture, which was referenced to 1,3,5-trimethoxybenzene as internal standard. Enantioselectivity determined by chiral SFC.

sertion of a Cu-phosphido into cyclopropenes, followed by protodemetalation, would generate chiral cyclopropyl phosphines (Figure 1C).[15]

We choose diphenyl phosphine (**2a**) and cyclopropene **1a** as model substrates. For the convenience of handling and analysis, the cyclopropyl phosphine products were oxidized with sulfur to generate the corresponding phosphine sulfides.[20] In previous studies using copper catalysis, Yin's group demonstrated the superiority of Taniaphos ligands for the Cu-catalyzed alkylation of secondary phosphines.[9g] However, Taniaphos ligands showed low enantioselectivity in this transformation (Table 1, entry 7). Instead, we found that the DuPhos ligand family is most promising (Table 1, entry 8, 9). Higher selectivity was correlated with larger R-substituents on the ligand (92% yield, 98:2 *er*) (see below). The addition of base is necessary to promote the formation of Cu-phosphido (Table 1, entry 3). With further tuning of the reaction stoichiometry, we developed a convenient and practical protocol for the asymmetric coupling of phosphines and cyclopropenes under Cu catalysis.

We demonstrated the utility of this Cu-catalyzed transformation with fifteen unique cyclopropenes bearing different functionalities with a range of electronic and steric properties as summarized in Table 2. High yields (81–93%) and stereoselectivities (96:4–97:3 *er*) are observed for cyclopropenes with electron-rich aromatic rings (**3ba**, **3ca**). An electron-poor aromatic ring (**3da**) gives good stereoselectivity (>20:1 *dr*, 98:2 *er*) and moderate yield (67%). Diphenyl phosphine (**2a**) successfully adds to cyclopropenes bearing more sterically hindered meta- (**3ea**) and ortho-substituted (**3fa**) aryl rings with slightly lower stereoselectivities (86:14–93:7 *er*, >20:1 *dr*). Substituents on the cyclopropene can be replaced with bulkier naphthyl (**3ga**) and ethyl groups (**3ha**). Cyclopropenes with alcohol (**3ia**) and methyl ether (**3ja**) substituents undergo the transformation with moderate yields (64–74%) and high stereoselectivities (>20:1 *dr*, 94:6 *er*). In addition, amide substituted cyclopropene (**3ka**) undergoes hydrophosphination (67% yield, >20:1 *dr*, 99:1 *er*). However, when the aryl group on cyclopropene is replaced with a benzyl group (**3la**), the reactivity (38%) and stereoselectivity (78:22 *er*, 1:1.3 *dr*) are both lowered. With this transformation, we also successfully prepared spirocyclic phosphine **3ma**.[21,22] Menthol ester cyclopropene (**3na**) gives moderate diastereoselectivity (5:1 *dr*). Ester bearing cyclopropenes (**3oa**, **3pa**) give excellent reactivity (75–85%) but lower stereoselectivities (87:13–89:11 *er*, >20:1–1:1.6 *dr*).

Our method encompasses a range of phosphine nucleophiles as shown in Table 3. Phosphines bearing electron donating Me, ^{t}Bu, and OMe groups at the para position (**3ab**, **3ac**, **3ad**) add to cyclopropenes (74–86%) with high enantioselectivities (96:4–98:2 *er*). Electron poor phosphines are well-tolerated (**3ae**). Even phosphines with ortho- substituted (**3af**, **3ag**), 3,5-substituted (**3ah**) and 3,4,5-substituted aromatic rings (**3ai**) transform in 65–78% yield and high enantioselectivities (93:7–98:2 *er*). This method tolerates heterocyclic phosphines, such as 2-furyl **2j**,

© 2023 Wiley-VCH GmbH

15213757, 2023, 36, Downloaded from https://onlinelibrary.wiley.com/doi/10.1002/ange.202306511 by University Of California - Irvine, Wiley Online Library on [05/06/2024]. See the Terms and Conditions (https://onlinelibrary.wiley.com/terms-and-conditions) on Wiley Online Library for rules of use; OA articles are governed by the applicable Creative Commons License

Table 2: Hydrophosphination of various cyclopropenes.[a]

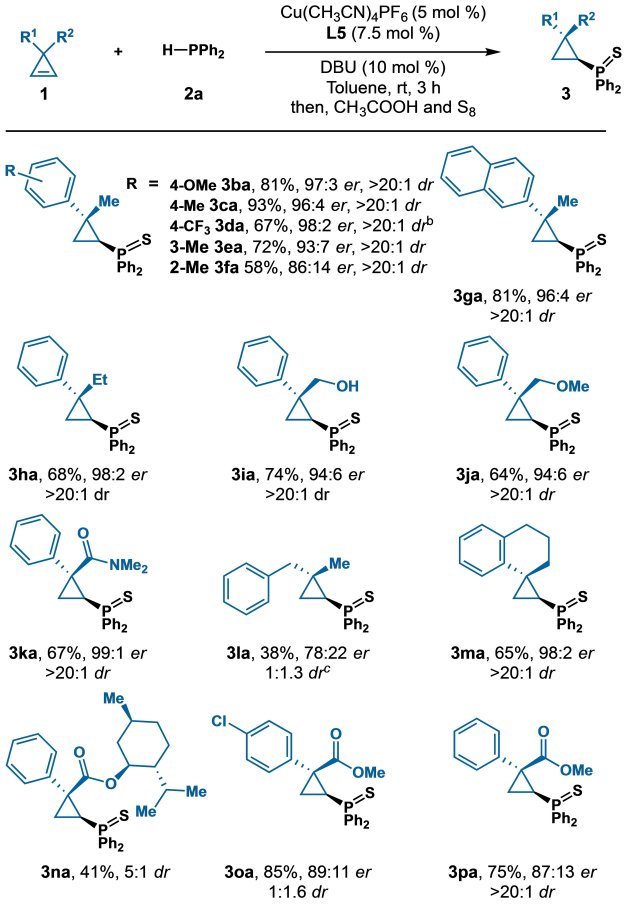

[a] Reaction conditions: **1** (0.12 mmol), **2a** (0.10 mmol), $Cu(CH_3CN)_4PF_6$ (5.0 mol%), ligand (7.5 mol%), DBU (10 mol%), toluene (0.40 mL), 3 h. Isolated yield of **3**. Diastereomeric ratios (*dr*) were determined from ^{1}H NMR analysis of the unpurified reaction mixture. Enantioselectivity determined by chiral SFC. [b] Reaction time is 24 hours. [c] inseparable diastereomers.

Table 3: Hydrophosphination of **1a** with various phosphines.[a]

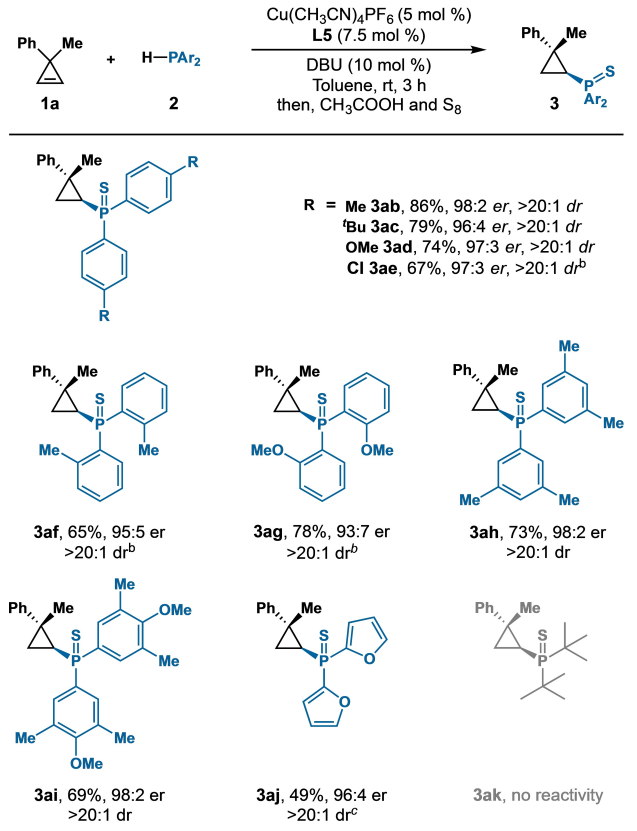

[a] Reaction conditions: **1** (0.12 mmol), **2a** (0.10 mmol), $Cu(CH_3CN)_4PF_6$ (5.0 mol%), ligand (7.5 mol%), DBU (10 mol%), toluene (0.40 mL), 3 h. Isolated yield of **3**. Diastereomeric ratios (*dr*) were determined from ^{1}H NMR analysis of the unpurified reaction mixture. Enantioselectivity determined by chiral SFC. [b] Reaction performed for 12 hours. [c] Reaction performed at 80 °C for 12 hours.

which gives **3aj** (49 % yield, 96:4 *er*) at elevated temperature (80 °C, 12 hours). However, alkyl substituted phosphine (**3ak**) failed to give any reactivity.

Based on literature precedent[9g,15d–e] and our own observations, we propose the general catalytic cycle in Figure 2A. Initially, $Cu(CH_3CN)_4PF_6$ binds to (*R*,*R*)-^{i}Pr-DuPhos to generate a mono(chelate) species **4** followed by the coordination of phosphine (**2**) and deprotonation to generate Cu-phosphido complex **5**. The novel step in the cycle involves addition of Cu-phosphido intermediate (**5**) to the cyclopropene (**1a**). We imagined that **5** could undergo either direct nucleophilic attack[23] or insertion into the cyclopropene π-bond.[24] Lastly, elimination of the copper catalyst regenerates **4** and releases cyclopropyl phosphine **3** to complete the catalytic cycle.

To investigate our proposed mechanism, we performed a series of experiments. These experiments were performed in THF which provided a completely homogeneous solution as compared to toluene. First, we obtained the rate law by variable time normalization analysis.[25] The fractional order was observed for diphenyl phosphine (**2a**), possibly because it involves other competitive pathways, and it is a strong coordinating compound that can act as a ligand to copper. We observed a first order dependance on the DBU concentration and a fractional order dependance on the copper catalyst concentration. In Yin's related study, the addition of a base (e.g., Barton's base) to a mixture of $Cu(CH_3CN)_4PF_6$, bidentate phosphine ligand,[9] and secondary phosphine results in a complicated mixture. In stark contrast, we found that addition of various bases (e.g., DBU, ^{t}BuOK, and Et_3N) to a mixture of $Cu(CH_3CN)_4PF_6$, (*R*,*R*)-^{i}Pr-DuPhos, and diphenyl phosphine results in immediate and selective formation of a new species on the basis of ^{31}P NMR. This species was isolated and further characterized by ^{31}P NMR and mass spec analysis and determined to be a Cu-phosphido dimer **7** (Figure 2B). In this dimer, the lone pair of the X-type phosphido ligand of **5** acts as an L-type ligand to form a η^2-bridge to another unit of Cu-DuPhos mono-chelate **4**. We propose this species to be the catalyst resting state. In line with this observation, our kinetics studies, and similar observations made by Appel and co-workers while studying copper hydride catalysis,[26] we propose the DBU acts as not only a base but also an L-

© 2023 Wiley-VCH GmbH

15213757, 2023, 36, Downloaded from https://onlinelibrary.wiley.com/doi/10.1002/ange.202306511 by University Of California - Irvine, Wiley Online Library on [05/06/2024]. See the Terms and Conditions (https://onlinelibrary.wiley.com/terms-and-conditions) on Wiley Online Library for rules of use; OA articles are governed by the applicable Creative Commons License

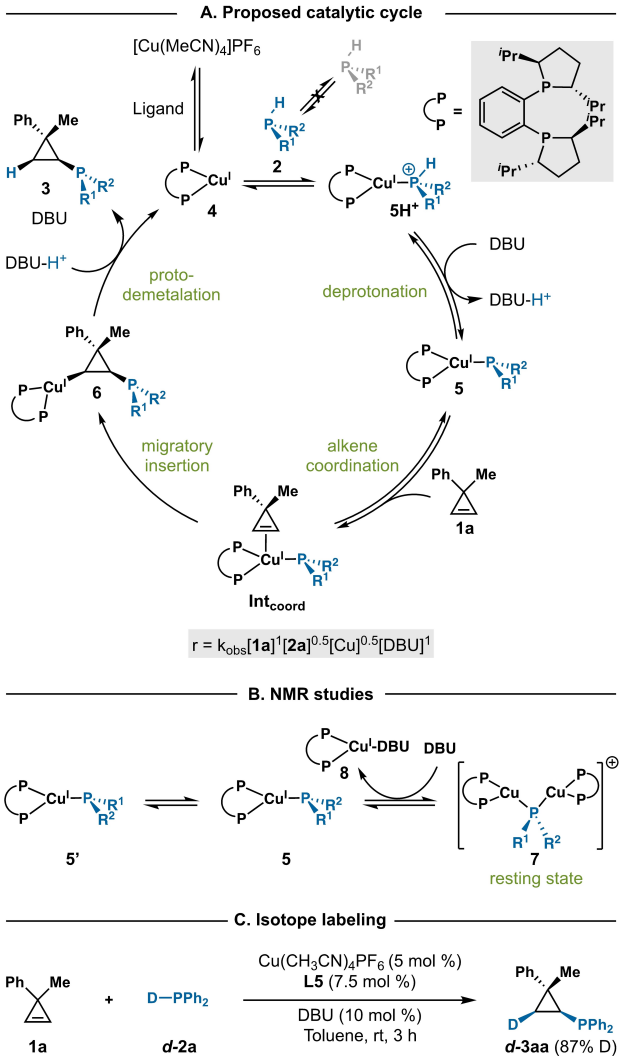

Figure 2. Proposed mechanism and experimental studies: **(A)** Proposed catalytic cycle for Cu-catalyzed hydrophosphination. **(B)** Observation of resting state by NMR studies. **(C)** Deuterium labeling study revealed *syn*-addition of P–D to cyclopropene double bond.

type ligand. The DBU undergoes ligand substitution with the dimeric resting state **7** to liberate the catalytically active monomeric Cu-phosphido **5**. This hypothesis is further supported by ^{31}P NMR studies which reveal decomposition of the dimer **7** in the presence of a large excess of DBU. Performing the transformation with isotopically labelled ***d*-2a** revealed that the hydrophosphination proceeds via a *syn*-addition of the P–D bond across the cyclopropene double bond (Figure 2C).[27]

With this mechanism in mind, we examined the possibility of setting a phosphorus stereocenter via a dynamic kinetic asymmetric transformation (DyKAT).[27] As outlined in the proposed mechanism, pyramidal inversion of the secondary phosphine is impractically slow at room temperature while epimerization of Cu-phosphido **5** with **5′** occurs rapidly.[15c–e,29] We subjected unsymmetrically substituted phosphine **2l** to the reaction conditions to test this hypothesis and observed a 3:1 *dr* for the cyclopropyl phosphine products and an *er* of 96:4 and 88:12 for the major and minor diastereomers respectively (Scheme 1). Based on our aforementioned results, we assume effective desymmetrization of the cyclopropene occurs with relatively low control over the configuration of the phosphorus stereocenter; these results are in line with a recent report from Glueck using a similar catalyst for asymmetric alkylation of secondary phosphines.[15e] On the basis of ^{31}P NMR studies, Glueck and co-workers were able to observe both Cu-phosphido diastereomers and measure the ratio of these phosphorus epimers (4:1 *dr*).[15d] In our case, the dimeric nature of the resting state renders the bridging phosphorus atom non-stereogenic, thwarting our attempts at a similar analysis.

To support the proposed mechanism and analyze the details for the enantioselective hydrophosphination of cyclopropenes, we performed a density functional theory (DFT) analysis on the title reaction of 3-methyl-3-phenylcyclopropene (**1a**) and diphenyl phosphine (**2a**) catalyzed by Cu-^{i}Pr-Duphos complex (**4**). DFT computations were performed utilizing ωB97XD/def2-TZVP PCM(toluene)//B97D/def2-SVP level of theory as implemented in Gaussian 16.[30–36] Thermal corrections were computed using Grimme's quasi-rigid rotor harmonic oscillator approximation.[37] IRC calculations were performed to confirm that transition structures (TSs) connected minima along the potential energy surface. A thorough exploration of the catalyst conformational space was performed using CREST. In addition, a detailed exploration of TS conformations was performed for the selectivity-determining step (see Supporting Information pages S35–36 for details).

Our computational study sought to identify both the turnover-limiting and stereoselectivity-determining steps of the catalytic cycle and to explain the origins of experimentally observed stereoselectivity. The potential energy surface for the lowest energy pathway resulting from our investigation is shown in Figure 3. The reaction is initiated via the coordination of diphenyl phosphine **2a** to Cu-Duphos to give the Cu–HPPh$_2^+$ complex **5aH$^+$**. Deprotonation of this cationic complex **5aH$^+$** by DBU is a low barrier step (**TS$_{Dep}$**, $\Delta G^{\ddagger}$ = 4.8 kcal/mol) that leads to the reversible formation of Cu-phosphido intermediate **5a** (chosen as the reference structure in the reaction coordinate). Following deprotonation, **5a** binds cyclopropene **1a** via π-coordination transition structure **TS$_{coord}$** ($\Delta G^{\ddagger}$ = 15.1 kcal/mol) to generate Cu-alkene complex **Int$_{coord}$**. The subsequent 1,2-migratory insertion into the cyclopropene π-bond (**TS$_{MI}$**) has a free energy barrier of 19.2 kcal/mol relative to **5a** and represents a highly exothermic step in the pathway, which results in a stable, significantly lower energy copper coordinated cyclopropyl phosphine intermediate **6a** residing 12.5 kcal/mol below the

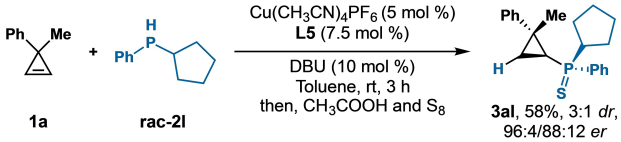

Scheme 1. Dynamic kinetic asymmetric transformation.

© 2023 Wiley-VCH GmbH

15213757, 2023, 36, Downloaded from https://onlinelibrary.wiley.com/doi/10.1002/ange.202306511 by University Of California - Irvine, Wiley Online Library on [05/06/2024]. See the Terms and Conditions (https://onlinelibrary.wiley.com/terms-and-conditions) on Wiley Online Library for rules of use; OA articles are governed by the applicable Creative Commons License

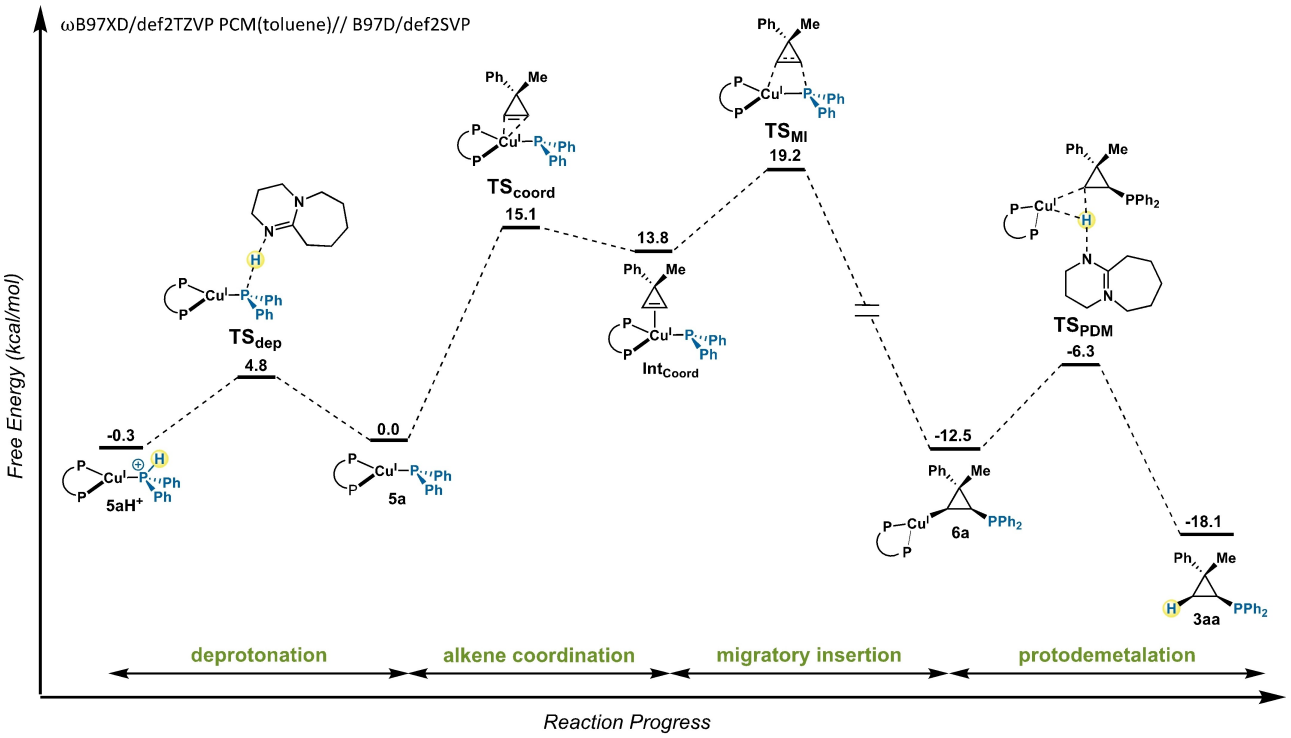

Figure 3. Reaction coordinate diagram depicting the relative barriers of deprotonation, alkene coordination, migratory insertion and protodemetalation in the hydrophosphination of cyclopropene. Migratory insertion is the stereoselectivity determining step.

monomeric resting state **5a**. The reaction pathway then proceeds through a facile stereo-retentive protodemetalation with a barrier of 6.2 kcal/mol ($\mathbf{TS_{PDM}}$, $\Delta G^{\ddagger} = -6.3$ kcal/mol relative to **5a**)—a copper mediated protonation from DBU occurs *syn* to the diphenyl phosphine substituent—to concomitantly regenerate **4** and afford the *syn*-hydrophosphinated cyclopropane product **3aa** (transferred proton shown in blue and highlighted in yellow).[38–40] This protodemetalation step ($\mathbf{TS_{PDM}}$) proceeds through a unique three-center, two-electron bond transition structure (C–Cu bond-breaking is 2.11 Å and C–H bond forming distance is 1.42 Å), consistent with the exclusive *syn* addition observed when the reaction is performed with *d*-**2a** (Figure 4 and Figure2 C) (vide supra). Incidentally, several alternative pathways for protodemetalation were also explored computationally (see Supporting Information page S37). A *syn*-protodemetalation TS analogous to $\mathbf{TS_{PDM}}$, whereby copper mediates the proton transfer from a protonated PPh_2 on the adjacent carbon, was found to be 25 kcal/mol higher in energy than $\mathbf{TS_{PDM}}$.

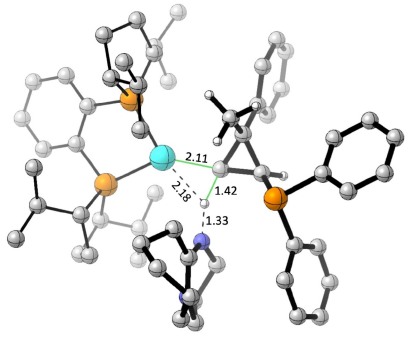

Figure 4. Three-center, two-electron bond transition structure for the product-forming *syn*-protodemetalation of Cu-Duphos from cyclopropene via DBU-H$^+$.

Analysis of the potential energy surface indicates that migratory insertion via $\mathbf{TS_{MI}}$ is the enantio- and diastereoselectivity-determining step in the hydrophosphination reaction. To investigate catalyst-substrate interactions that dictate the enantioselectivity in this reaction, a conformational search was conducted on $\mathbf{TS_{MI}}$ for transition structures that lead to the formation of both the major and minor enantiomers of **3aa**. The lowest energy transition structure which leads to the major enantiomer (Figure 5A, $\mathbf{TS_{MI\text{-}Major}}$) is favored by 2.1 kcal/mol with respect to the lowest energy structure leading to the minor enantiomer (Figure 5A, $\mathbf{TS_{MI\text{-}Minor}}$). At 298 K, a $\Delta\Delta G^{\ddagger}$ of 2.1 kcal/mol corresponds to a predicted *er* of 97.5:2.5, which is in excellent agreement with the experimental *er* of 98:2 ($\Delta\Delta G^{\ddagger}$ of 2.3 kcal/mol) for the title reaction.

To further evaluate the origin of enantioselectivity, a distortion-interaction analysis was performed on $\mathbf{TS_{MI\text{-}Major}}$ and $\mathbf{TS_{MI\text{-}Minor}}$.[41–43] Distortion energy describes the energy required to distort reactants and catalysts from their respective ground states into the necessary transition state conformations. Energy decomposition reveals that the major enantiomer suffers a greater degree of distortion energy, 2.4 kcal/mol ($\Delta\Delta E^{\ddagger}$) more than the minor enantiomer (Fig-

© 2023 Wiley-VCH GmbH

15213757, 2023, 36, Downloaded from https://onlinelibrary.wiley.com/doi/10.1002/ange.202306511 by University Of California - Irvine, Wiley Online Library on [05/06/2024]. See the Terms and Conditions (https://onlinelibrary.wiley.com/terms-and-conditions) on Wiley Online Library for rules of use; OA articles are governed by the applicable Creative Commons License

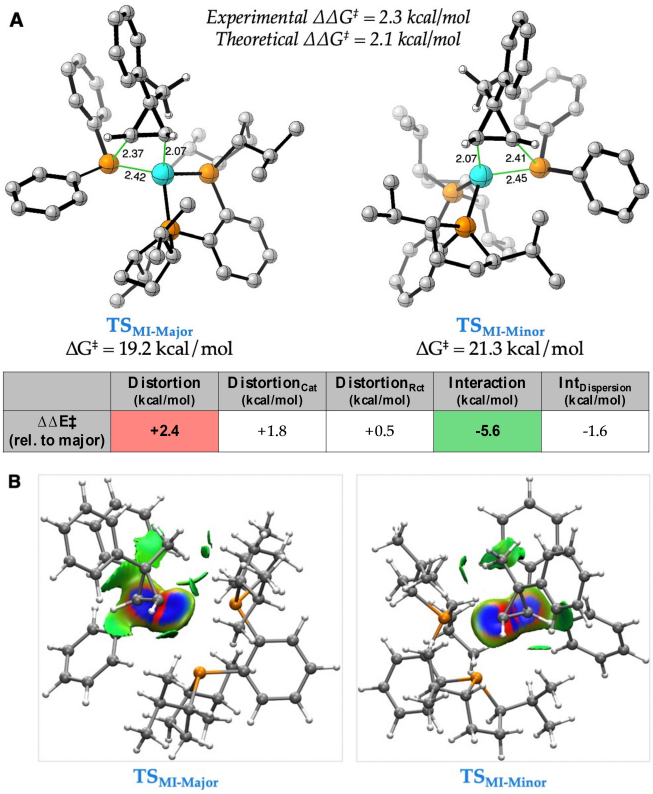

	Distortion (kcal/mol)	Distortion$_{Cat}$ (kcal/mol)	Distortion$_{Rct}$ (kcal/mol)	Interaction (kcal/mol)	Int$_{Dispersion}$ (kcal/mol)
ΔΔE‡ (rel. to major)	+2.4	+1.8	+0.5	-5.6	-1.6

Figure 5. **(A)** Lowest energy TSs of the enantioselectivity-determining step with experimental and theoretical free energy barriers after Boltzmann weighting. Also shown are components of the energy decomposition analysis relative to the major enantiomer. ΔDistortion of the catalyst (Cat) and reactants (*R*ct) versus overall ΔInteraction (including ΔDispersion) are highlighted. **(B)** Non-covalent interaction (NCI) plots depict dispersive interactions (shown in green) between Cu-DuPhos and PPh_2 with cyclopropene reactant for each TS leading to the major and minor enantiomers of the product (isosurface 0.009). Red and blue coloring in the NCI plot indicate areas of strongly attractive or repulsive interactions, while the green indicates areas of weakly attractive dispersion interactions.

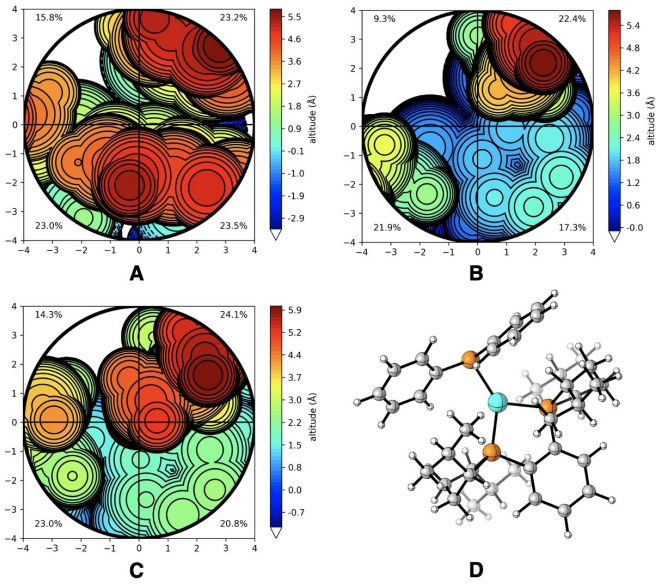

Figure 6. Steric maps depicting the catalytic pocket prior to coordination of cyclopropene when the ligand on copper is **(A)** R-SEGPHOS (**L1**), **(B)** (R,R)-Me-DuPhos (**L3**), or **(C)** (R,R)-^{i}Pr-DuPhos (**L5**). The orientation of the copper-phosphido complexes in these steric maps is depicted in **D**.

ure 5A). The majority (1.8 kcal/mol) of this 2.4 kcal/mol difference in distortion energy arises from the distortion of the diphenyl phosphine and Cu-DuPhos catalyst, while the remaining 0.6 kcal/mol arises from distortion of the cyclopropene substrate. Despite distortion energy favoring the minor enantiomer, advantageous interaction energy favors the major enantiomer by 5.6 kcal/mol. Interaction energy describes how the distorted catalyst and reactant fragments interact with one another within the TS, a portion of this can be accounted for as dispersion energy. The major enantiomer exhibits favorable dispersions in the form of significant CH—π interactions between the diphenyl phosphine and the cyclopropene methyl group as well as moderate dispersions amongst the Cu-DuPhos isopropyl groups and the cyclopropene substrate (Figure 5B).[44,45] A visual comparison of the dispersion interactions in the enantioselectivity-determining transition structures shows that $\mathbf{TS_{MI\text{-}major}}$ enjoys more stabilizing dispersion interactions than $\mathbf{TS_{MI\text{-}minor}}$ (as evidenced by the green areas in the non-covalent interaction (NCI) plots of the two TSs shown in Figure 5B).[46,47] In addition to the favorable dispersions imparted by the isopropyl groups in $\mathbf{TS_{MI\text{-}Major}}$, the Cu-DuPhos catalyst also serves to add steric bulk to the catalytic pocket, blocking more than three-fourths of the pocket when coordinated to PPh_2, forcing the cyclopropene substrate to bind in the same pocket for both enantiomers (see Supporting Information page S38).

From this analysis, steric interactions have been identified to play a key role in controlling stereoselectivity. Using this information, the buried volume and steric maps for intermediate **5a** with **L1**, **L3**, **L4** and **L5** as ligands were investigated.[48–49] The buried volume analysis reveals that ligand **L1** (Figure 6A) has a slightly smaller available free volume compared to the best ligand **L5** (Figure 6C). However, **L5** is more fluctional compared to the rigid biphenyl backbone of **L1**, thereby accommodating the incoming cyclopropene more readily. Plausibly leading to an overall reduction in the background reaction of **L5**, compared to **L1**, thus enabling better enantioselectivity in **L5**. Similarly, despite having the same backbone as **L5** (R = ^{i}Pr), ligands **L3** (R=Me, Figure 6B) and **L4** (R=Et) have more available free volume, leading to reduced steric control and slightly lower enantioselectivity.[50]

Conclusion

In conclusion, we report asymmetric hydrophosphination of cyclopropenes in high enantio- and diastereoselectivity. Mechanistic studies reveal an unusual dimeric resting state and a surprising rate enhancement effect from DBU, which plays an important role in forming the catalytically active monomer. Proof of concept for enrichment of phosphorus

© 2023 Wiley-VCH GmbH

15213757, 2023, 36, Downloaded from https://onlinelibrary.wiley.com/doi/10.1002/ange.202306511 by University Of California - Irvine, Wiley Online Library on [05/06/2024]. See the Terms and Conditions (https://onlinelibrary.wiley.com/terms-and-conditions) on Wiley Online Library for rules of use; OA articles are governed by the applicable Creative Commons License

stereocenters is demonstrated through a DyKAT of an unsymmetrically substituted secondary phosphine. Both the enantio- and diastereoselectivity of the product are determined during the migratory insertion step. An analysis of the relevant TSs indicate that selectivity is controlled by a combination of dispersion and steric interactions. These insights will guide future studies on developing methods to set phosphorus stereocenters and design both mono- and bidentate phosphine ligands. These studies help advance our understanding of copper catalysis, hydrofunctionalization, and phosphine synthesis.

Supporting Information

The authors have cited additional references within the Supporting Information.[51–54]

AcknowledgementsReferences

VMD acknowledges the National Science Foundation (under the NSF Grant No. [2247923]) and National Institutes of Health (R35GM127071). JSH acknowledges the National Institute of General Medicine NIH R35GM147183 as well as the XSEDE Science Gateway Program (under the NSF Grant Numbers ACI-1548562, CHE180061). We thank Solvias AG for donating commercial ligands and phosphine compounds used in the phosphine scope.

Conflict of Interest

The authors declare no conflict of interest.

Data Availability Statement

The data that support the findings of this study are available in the supplementary material of this article.

Keywords: Asymmetric Catalysis · Copper-Phosphido · Cyclopropenes · Hydrophosphination

[1] a) Q. L. Zhou, in *Privileged Chiral Ligands and Catalysts, Vol. 6*, Wiley-VCH, Weinheim, **2011**; b) G. P. Horsman, D. L. Zechel, *Chem. Rev.* **2017**, *117*, 5704; c) H. Ni, W. L. Chan, Y. Lu, *Chem. Rev.* **2018**, *118*, 9344; d) V. Iaroshenko, in *Organophosphorus Chemistry: from Molecules to Applications*, Wiley-VCH, Weinheim, **2019**.

[2] V. Devreux, J. Wiesner, J. L. Goeman, J. Van der Eycken, H. Jomaa, S. Van Calenbergh, *J. Med. Chem.* **2006**, *49*, 2656.

[3] K. Suzuki, Y. Hori, Y. Nakayama, T. Kobayashi, *J. Synth. Org. Chem. Jpn.* **2011**, *69*, 1231.

[4] For selected examples of hydrophosphination, see: a) A. Togni, H. Grützmacher, in *Catalytic Heterofunctionalization: From Hydroamination to Hydrozironation*, Wiley-VCH, Weinheim, **2001**, p. 143; b) L. Rosenberg, *ACS Catal.* **2013**, *3*, 2845; c) C. A. Bange, R. Waterman, *Chem. Eur. J.* **2016**, *22*, 12598; d) D. S. Glueck, *J. Org. Chem.* **2020**, *85*, 14276; e) K. D. Troev, in *Reactivity of PH Group of Phosphorus Based Compounds*, Academic Press, San Diego, **2017**, p. 19; f) R. G. Belli, J. Yang, E. N. Bahena, R. McDonald, L. Rosenberg, *ACS Catal.* **2022**, *12*, 5247; g) B. T. Novas, R. Waterman, *ChemCatChem* **2022**, *14*, e202200988; h) Y. Zhang, Y. Jiang, M. Li, Z. Huang, J. Wang, *Chem Catalysis* **2022**, *2*, 3163.

[5] B. M. Trost, *Science* **1991**, *254*, 1471.

[6] a) S. A. Pullarkat, P. H. Leung, *Chiral Metal Complex-Promoted Asymmetric Hydrophosphinations in Topics in Organometallic Chemistry, Vol. 43*, Springer, Berlin, Heidelberg, **2013**, p. 145; b) S. A. Pullarkat, *Synthesis* **2016**, *48*, 493; c) R. J. Chew, P. H. Leung, *Chem. Rec.* **2016**, *16*, 141.

[7] a) B. Join, D. Mimeau, O. Delacroix, A. C. Gaumont, *Chem. Commun.* **2006**, *30*, 3249; b) X. T. Liu, X. Y. Han, Y. Wu, Y. Y. Sun, L. Gao, Z. Huang, Q. W. Zhang, *J. Am. Chem. Soc.* **2021**, *143*, 11309.

[8] a) A. Sadeer, Y. J. Ong, T. Kojima, C. Q. Foo, Y. Li, S. A. Pullarkat, P. H. Leung, *Chem. Asian J.* **2018**. *13*, 2829; b) Z. Lu, H. Zhang, Z. Yang, N. Ding, L. Meng, J. Wang, *ACS Catal.* **2019**, *9*, 1457.

[9] a) I. Kovacik, D. K. Wicht, N. S. Grewal, D. S. Glueck, C. D. Incarvito, I. A. Guzei, A. L. Rheingold, *Organometallics* **2000**, *19*, 950; b) A. D. Sadow, I. Haller, L. Fadini, A. Togni, *J. Am. Chem. Soc.* **2004**, *126*, 14704; c) J. J. Feng, X. F. Chen, M. Shi, W. L. Duan, *J. Am. Chem. Soc.* **2010**, *132*, 5562; d) Y.-H. Huang, S. A. Pullarkat, Y.-X. Li, P. H. Leung, *Inorg. Chem.* **2012**, *51*, 2533; e) Y.-R. Chen, J.-J. Feng, W.-L. Duan, *Tetrahedron Lett.* **2014**, *55*, 595; f) R. H. X. Teo, H. G. J. Chen, Y.-X. Li, P. A. Pullarkat, P. K. Leung, *Adv. Synth. Catal.* **2020**, *362*, 2373; g) Y.-B. Li, H. Tian, L. Yin, *J. Am. Chem. Soc.* **2020**, *142*, 20098; h) W.-J. Yue, J.-Z. Xiao, S. Zhang, L. Yin, *Angew. Chem. Int. Ed.* **2020**, *59*, 7057; i) C.-Y. Wang, K.-S. Huang, J. Ye, W.-L. Duan, *J. Am. Chem. Soc.* **2021**, *143*, 5685; j) J. M. Pérez, R. Postolache, M. Castiñeira Reis, E. G. Sinnema, D. Vargová, F. Vries, E. Otten, L. Ge, S. R. Harutyunyan, *J. Am. Chem. Soc.* **2021**, *143*, 20071; k) L. Ge, S. R. Harutyunyan, *Chem. Sci.* **2022**, *13*, 1307.

[10] a) R. D. Bach, O. Dmitrenko, *J. Am. Chem. Soc.* **2004**, *126*, 4444; b) K. B. Wiberg, *Angew. Chem. Int. Ed. Engl.* **1986**, *25*, 312–322.

[11] a) N. Y. Demjanov, M. N. Doyarenko, *Bull. Acad. Sci. Russ.* **1922**, *16*, 297; b) F. L. Carter, V. L. Frampton, *Chem. Rev.* **1964**, *64*, 497; c) G. L. Closs, *Adv. Alicyclic Chem.* **1966**, *1*, 53; d) M. S. Baird, *Chem. Rev.* **2003**, *103*, 1271; e) R. Walsh, *Chem. Soc. Rev.* **2005**, *34*, 714; f) M. Rubin, M. Rubina, V. Gevorgyan, *Synthesis* **2006**, *8*, 1221; g) M. Rubin, M. Rubina, V. Gevorgyan, *Chem. Rev.* **2007**, *107*, 3117; h) Z.-B. Zhu, Y. Wei, M. Shi, *Chem. Soc. Rev.* **2011**, *40*, 5534; i) R. Vicente, *Synthesis* **2016**, *48*, 2343; j) B. Prasad Raiguru, S. Nayak, D. Ranjan Mishra, T. Das, S. Mohapatra, N. Priyadarsini Mishra, *Asian J. Org. Chem.* **2020**, *9*, 1088; k) P.-H. Li, X.-Y. Zhang, M. Shi, *Chem. Commun.* **2020**, *56*, 5457; l) Y. Cohen, I. Marek, *Org. Lett.* **2019**, *21*, 9162.

[12] For selected examples for hydrofunctionalization of cyclopropenes, see: a) L.-Y. Dian, I. Marek, *Chem. Rev.* **2018**, *118*, 8415; b) M. Rubina, M. Rubin, V. Gevorgyan, *J. Am. Chem. Soc.* **2003**, *125*, 7198; c) M. Rubina, M. Rubin, V. Gevorgyan, *J. Am. Chem. Soc.* **2004**, *126*, 3688; d) W. M. Sherrill, M. Rubin, *J. Am. Chem. Soc.* **2008**, *130*, 13804; e) D. H. T. Phan, K. G. M. Kou, V. M. Dong, *J. Am. Chem. Soc.* **2010**, *132*, 16354; f) F. Liu, X. Bugaut, M. Schedler, R. Fröhlich, F. Glorius, *Angew. Chem. Int. Ed.* **2011**, *50*, 12626; g) H.-L. Teng, Y. Luo, B. Wang, L. Zhang, M. Nishiura, Z. Hou, *Angew. Chem. Int. Ed.* **2016**, *55*, 15406; h) A. Parra, L. Amenós, M. Guisán-Ceinos, A. López, J. L. G. Ruano, M. Tortosa, *J. Am. Chem. Soc.* **2014**, *136*, 15833; i) Z. Li, J. Zhao, B. Sun, T. Zhou, M. Liu, S. Liu,

© 2023 Wiley-VCH GmbH

15213757, 2023, 36, Downloaded from https://onlinelibrary.wiley.com/doi/10.1002/ange.202306511 by University Of California - Irvine, Wiley Online Library on [05/06/2024]. See the Terms and Conditions (https://onlinelibrary.wiley.com/terms-and-conditions) on Wiley Online Library for rules of use; OA articles are governed by the applicable Creative Commons License

M. Zhang, Q. Zhang, *J. Am. Chem. Soc.* **2017**, *139*, 11702; j) Y. Luo, H.-L. Teng, M. Nishiura, Z. Hou, *Angew. Chem. Int. Ed.* **2017**, *56*, 9207; k) L. Dian, I. Marek, *Angew. Chem. Int. Ed.* **2018**, *57*, 3682; l) H. Zhang, W. Huang, T. Wang, F. Meng, *Angew. Chem. Int. Ed.* **2019**, *58*, 11049; m) G. Zheng, Z. Zhou, G. Zhu, S. Zhai, H. Xu, X. Duan, W. Yi, X. Li, *Angew. Chem. Int. Ed.* **2020**, *59*, 2890; n) W. Huang, F. Meng, *Angew. Chem. Int. Ed.* **2021**, *60*, 2694; o) L. Dian, I. Marek, *Org. Lett.* **2020**, *22*, 4914; p) S.-Z. Nie, A. Lu, E. L. Kuker, V. M. Dong, *J. Am. Chem. Soc.* **2021**, *143*, 6176; q) R. Yu, S.-Z. Cai, C. Li, X. Fang, *Angew. Chem. Int. Ed.* **2022**, *61*, e202200733; r) Q. Huang, Y. Chen, X. Zhou, L. Dai, Y. Lu, *Angew. Chem. Int. Ed.* **2022**, *61*, e202210560.

[13] J.-N. Li, L. Liu, Y. Fu, Q.-X. Guo, *Tetrahedron* **2006**, *62*, 4453.

[14] a) L.-B. Han, C.-Q. Zhao, S. Onozawa, M. Goto, M. Tanaka, *J. Am. Chem. Soc.* **2002**, *124*, 3842; b) Q. Xu, L.-B. Han, *Org. Lett.* **2006**, *8*, 2099; c) R. Beaud, R. J. Phipps, M. J. Gaunt, *J. Am. Chem. Soc.* **2016**, *138*, 13183; d) S.-Z. Nie, R. T. Davison, V. M. Dong, *J. Am. Chem. Soc.* **2018**, *140*, 16450; e) B. M. Trost, S. M. Spohr, A. B. Rolka, C. A. Rolka, *J. Am. Chem. Soc.* **2019**, *141*, 14098; f) Z. Yang, X. Gu, L.-B. Han, J. Wang, *Chem. Sci.* **2020**, *11*, 7451; g) Q. Dai, L. Liu, Y. Qian, W. Li, J. Zhang, *Angew. Chem. Int. Ed.* **2020**, *59*, 20645; h) Z. Yang, J. Wang, *Angew. Chem. Int. Ed.* **2021**, *60*, 27288; i) Q. Zhang, X.-T. Liu, Y. Wu, Q.-W. Zhang, *Org. Lett.* **2021**, *23*, 8683; j) B. Li, M. Liu, S. U. Rehman, C. Li, *J. Am. Chem. Soc.* **2022**, *144*, 2893; k) H. Wang, H. Qian, J. Zhang, S. Ma, *J. Am. Chem. Soc.* **2022**, *144*, 12619; l) B. K. Alnasleh, W. M. Sherrill, M. Rubin, *Org. Lett.* **2008**, *10*, 3231.

[15] For selected example of metal-phosphido chemistry, see: a) G. C. Fortman, A. M. Z. Slawin, S. P. Nolan, *Organometallics* **2010**, *29*, 3966; b) B. K. Najafabadi, J. F. Corrigan, *Dalton Trans.* **2015**, *44*, 14235; c) G. Wang, S. K. Gibbons, D. S. Glueck, C. Sibbald, J. T. Fleming, L. J. Higham, A. L. Rheingold, *Organometallics* **2018**, *37*, 1760; d) S. K. Gibbons, C. R. D. Valleau, J. L. Peltier, M. F. Cain, R. P. Hughes, D. S. Glueck, J. A. Golen, A. L. Rheingold, *Inorg. Chem.* **2019**, *58*, 8854; e) S. K. Gallant, R. M. Tipker, D. S. Glueck, *Organometallics* **2022**, *41*, 1721; f) J. R. Moncarz, N. F. Laritcheva, D. S. Glueck, *J. Am. Chem. Soc.* **2002**, *124*, 13356; g) N. F. Blank, J. R. Moncarz, T. J. Brunker, C. Scriban, B. J. Anderson, O. Amir, D, S. Glueck, L. N. Zakharov, J. A. Golen, C. D. Incarvito, A. L. Rheingold, *J. Am. Chem. Soc.* **2007**, *129*, 6847; h) V. S. Chan, I. C. Stewart, R. G. Bergman, F. D. Toste, *J. Am. Chem. Soc.* **2006**, *128*, 2786; i) V. S. Chan, R. G. Bergman, F. D. Toste, *J. Am. Chem. Soc.* **2007**, *129*, 15122; j) V. S. Chan, M. Chiu, R. G. Bergman, F. D. Toste, *J. Am. Chem. Soc.* **2009**, *131*, 6021; k) Q. Yang, J. Zhou, J. Wang, *Chem. Sci.* **2023**, *14*, 4413; l) S. Zhang, J. Xiao, Y. Li, C. Shi, L. Yin, *J. Am. Chem. Soc.* **2021**, *143*, 9912; m) Y.-B. Li, H. Tian, S. Zhang, J.-Z. Xiao, L. Yin, *Angew. Chem. Int. Ed.* **2022**, *61*, e202117760.

[16] Z.-Y. Li, G.-C. Peng, J.-B. Zhao, Q. Zhang, *Org. Lett.* **2016**, *18*, 4840.

[17] We identified a related protocol using $Pd(OAc)_2$ and (R)-SEGPHOS that is complementary to Wang's method. The transformation provides cyclopropyl phosphine **3aa** in 86% yield with 97:3 er. With these Pd conditions, we also obtained p-chloro-phenyl ester cyclopropyl phosphine **3oa** (84%, 96:4 er, >20:1 dr) and phenyl ester cyclopropyl phosphine **3pa** (68%, 94:6 er, 9:1 dr) (see Supporting Information 2B for details).

[18] C. Torborg, M. Beller, *Adv. Synth. Catal.* **2009**, *351*, 3027.

[19] a) R. M. Bullock, J. G. Chen, L. Gagliardi, P. J. Chirik, O. K. Farha, C. H. Hendon, C. W. Jones, J. A. Keith, J. Klosin, S. D. Minteer, R. H. Morris, A. T. Radosevich, T. B. Rauchfuss, N. A. Strotman, A. Vojvodic, T. R. Ward, J. Y. Yang, Y. Surendranath, *Science* **2020**, *369*, eabc3183; b) J. Chen, L. Zhan, *Org. Chem. Front.* **2018**, *5*, 260; c) A. A. Toutov, W. Liu, K. N. Betz, A. Fedorov, B. M. Stoltz, R. H. Grubbs, *Nature* **2015**, *518*, 80.

[20] Deposition numbers 2100976 (for **3aa**) and 2154097 for (**3pa**) contain the supplementary crystallographic data for this paper. These data are provided free of charge by the joint Cambridge Crystallographic Data Centre and Fachinformationszentrum Karlsruhe Access Structures service. The absolute configurations of the remaining cyclopropyl phosphine sulfides **3** are assigned by analogy.

[21] P.-W. Xu, J.-S. Yu, C. Chen, Z.-Y. Cao, F. Zhou, J. Zhou, *ACS Catal.* **2019**, *9*, 1820.

[22] R. Rios, *Chem. Soc. Rev.* **2012**, *41*, 1060.

[23] a) A. Edwards, M. Rubina, M. Rubin, *Curr. Org. Chem.* **2016**, *20*, 1862; b) J. M. Fox, N. Yan, *Curr. Org. Chem.* **2005**, *9*, 719; c) B. M. Alnasleh, W. M. Sherrill, M. Rubina, J. Banning, M. Rubin, *J. Am. Chem. Soc.* **2009**, *131*, 6906.

[24] a) V. P. Ananikov, I. P. Beletskaya, *Chem. Asian J.* **2011**, *6*, 1423; b) K. M. E. Burton, D. A. Pantazis, R. G. Belli, R. McDonald, L. Rosenberg, *Organometallics* **2016**, *35*, 3970.

[25] J. Burés, *Angew. Chem. Int. Ed.* **2016**, *55*, 2028.

[26] C. M. Zall, J. C. Linehan, A. M. Appel, *J. Am. Chem. Soc.* **2016**, *138*, 9968.

[27] Y. Yamamoto, *J. Org. Chem.* **2018**, *83*, 12775.

[28] J. Steinreiber, K. Faber, H. Griengl, *Chem. Eur. J.* **2008**, *14*, 8060.

[29] W. E. Buhro, B. D. Zwick, S. Georgiou, J. P. Hutchinson, J. A. Gladysz, *J. Am. Chem. Soc.* **1988**, *110*, 2427.

[30] J. D. Chai, M. Head-Gordon, *Phys. Chem. Chem. Phys.* **2008**, *10*, 6615.

[31] S. Grimme, *J. Comput. Chem.* **2006**, *27*, 1787.

[32] A. Becke, *J. Chem. Phys.* **1997**, *107*, 8554.

[33] F. Weigend, R. Ahlrichs, *Phys. Chem. Chem. Phys.* **2005**, *7*, 3297.

[34] S. Miertus, E. Scrocco, Tomasi, *J. Chem. Phys.* **1981**, *55*, 117.

[35] J. Tomasi, B. Mennucci, R. Cammi, *Chem. Rev.* **2005**, *105*, 2999.

[36] M. J. Frisch, G. W. Trucks, H. B. Schlegel, G. E. Scuseria, M. A. Robb, J. R. Cheeseman, G. Scalmani, V. Barone, G. A. Petersson, H. Nakatsuji, X. Li, M. Caricato, A. V. Marenich, J. Bloino, B. G. Janesko, R. Gomperts, B. Mennucci, H. P. Hratchian, J. V. Ortiz, A. F. Izmaylov, J. L. Sonnenberg, Williams, F. Ding, F. Lipparini, F. Egidi, J. Goings, B. Peng, A. Petrone, T. Henderson, D. Ranasinghe, V. G. Zakrzewski, J. Gao, N. Rega, G. Zheng, W. Liang, M. Hada, M. Ehara, K. Toyota, R. Fukuda, J. Hasegawa, M. Ishida, T. Nakajima, Y. Honda, O. Kitao, H. Nakai, T. Vreven, K. Throssell, J. A. Jr. Montgomery, J. E. Peralta, F. Ogliaro, M. J. Bearpark, J. J. Heyd, E. N. Brothers, K. N. Kudin, V. N. Staroverov, T. A. Keith, R. Kobayashi, J. Normand, K. Raghavachari, A. P. Rendell, J. C. Burant, S. S. Iyengar, J. Tomasi, M. Cossi, J. M. Millam, M. Klene, C. Adamo, R. Cammi, J. W. Ochterski, R. L. Martin, K. Morokuma, O. Farkas, J. B. Foresman, D. J. Fox, *Gaussian 16*; Rev. C.01: Wallingford, CT, 2016.

[37] R. F. Ribeiro, A. V. Marenich, C. J. Cramer, D. G. Truhlar, *J. Phys. Chem. B* **2011**, *115*, 14556.

[38] M. L. O'Duill, K. M. Engle, *Synthesis* **2018**, *50*, 4699.

[39] Y. Yao, X. Zhang, S. Ma, *Org. Chem. Front.* **2020**, *7*, 2047.

[40] X. Yuan, D. Li, S. Wang, Y. Jiang, P. Liu, S. Bi, *J. Org. Chem.* **2022**, *87*, 11681.

[41] F. M. Bickelhaupt, K. N. Houk, *Angew. Chem. Int. Ed. Engl.* **2017**, *56*, 10070.

[42] D. H. Ess, K. N. Houk, *J. Am. Chem. Soc.* **2007**, *129*, 10646.

[43] R. Maji, S. C. Mallojjala, S. E. Wheeler, *Chem. Soc. Rev.* **2018**, *47*, 1142.

© 2023 Wiley-VCH GmbH

15213757, 2023, 36, Downloaded from https://onlinelibrary.wiley.com/doi/10.1002/ange.202306511 by University Of California - Irvine, Wiley Online Library on [05/06/2024]. See the Terms and Conditions (https://onlinelibrary.wiley.com/terms-and-conditions) on Wiley Online Library for rules of use; OA articles are governed by the applicable Creative Commons License

[44] G. Lu, R. Y. Liu, Y. Yang, C. Fang, D. S. Lambrecht, S. L. Buchwald, P. Liu, *J. Am. Chem. Soc.* **2017**, *139*, 16548.
[45] Y. Xi, B. Su, X. Qi, S. Pedram, P. Liu, J. F. Hartwig, *J. Am. Chem. Soc.* **2020**, *142*, 18213.
[46] T. Lu, Q. Chen, *J. Comput. Chem.* **2022**, *43*, 539.
[47] T. Lu, F. Chen, *J. Comput. Chem.* **2012**, *33*, 580.
[48] L. Falivene, Z. Cao, A. Petta, L. Serra, A. Poater, R. Oliva, V. Scarano, L. Cavallo, *Nat. Chem.* **2019**, *11*, 872.
[49] A. J. Schaefer, V. M. Ingman, S. E. Wheeler, *J. Comput. Chem.* **2021**, *42*, 1750.
[50] There is little difference between the buried volumes of L3 and L4, corresponding with the little difference in the observed ee for L3 and L4 (see Supporting Information Table S2 for buried volumes and all steric maps).
[51] W. M. Sherrill, R. Kim, M. Rubin, *Tetrahedron* **2008**, *64*, 8610.
[52] Z.-W. Chen, Y. Aota, H. M. H. Nguyen, V. M. Dong, *Angew. Chem. Int. Ed.* **2019**, *58*, 4705.
[53] N. I. Rinehart, A, J. Kendall, D. R. Tyler, *Organometallics* **2018**, *37*, 182.
[54] C. Y. Legault, CYLview, 1.0b; Université de Sherbrooke, **2009** (www.cylview.org).

Manuscript received: May 9, 2023
Accepted manuscript online: June 18, 2023
Version of record online: July 21, 2023

© 2023 Wiley-VCH GmbH

15213757, 2023, 36, Downloaded from https://onlinelibrary.wiley.com/doi/10.1002/ange.202306511 by University Of California - Irvine, Wiley Online Library on [05/06/2024]. See the Terms and Conditions (https://onlinelibrary.wiley.com/terms-and-conditions) on Wiley Online Library for rules of use; OA articles are governed by the applicable Creative Commons License